POLITECNICO DI TORINO
Repository ISTITUZIONALE

Composite Electrospun Fibers Containing Optimized B- and Cu-Doped Bioactive Glass Sol-Gel Particles for Potential Soft Tissue Engineering Applications

Original
Composite Electrospun Fibers Containing Optimized B- and Cu-Doped Bioactive Glass Sol-Gel Particles for Potential Soft Tissue Engineering Applications / Piatti, E., Miola, M., Liverani, L., Sartori, P., Vernè, Enrica., Boccaccini, A.R.. - In: ADVANCED ENGINEERING MATERIALS. - ISSN 1527-2648. - ELETTRONICO. - 28:4(2026), pp. 1-13. [10.1002/adem.202500946]

Availability:
This version is available at: 11583/3008683 since: 2026-03-12T11:24:26Z

Publisher:
Wiley

Published
DOI:10.1002/adem.202500946

Terms of use:

This article is made available under terms and conditions as specified in the corresponding bibliographic description in the repository

Publisher copyright

(Article begins on next page)

19 November 2026

ADVANCED ENGINEERING MATERIALS
www.aem-journal.com

Composite Electrospun Fibers Containing Optimized B- and Cu-Doped Bioactive Glass Sol-Gel Particles for Potential Soft Tissue Engineering Applications

Elisa Piatti, Marta Miola, Liliana Liverani, Paolo Sartori, Enrica Verné,* and Aldo R. Boccaccini*

Electrospinning (ES) is largely used to produce polymeric nano- and microfibers for various applications, including the biomedical fields. ES enables the production of biomimetic fibrous composite scaffolds that resemble the morphology of the extracellular matrix (ECM) of human tissues. However, literature lacks research on composite electrospun fiber tissue engineering (TE). The synergistic effect of biologically active ions with multitarget activity, in comparison to single-target approaches, is also underexplored. In this work, composite fibers based on poly(ε-caprolactone) (PCL) incorporating spherical sol-gel B- and Cu-doped bioactive glass (BG) particles, with potential use in soft TE, are fabricated and characterized with scanning electron microscopy, energy-dispersive X-ray spectroscopy, Fourier-transform infrared spectroscopy, contact angle measurements, acellular bioactivity, and mechanical and preliminary cell tests. The composite fibers are obtained by using benign solvents for the ES. The results showed good retention of the BG particles inside the PCL matrix, leading to bioactive behavior. Preliminary *in vitro* cellular tests with bone marrow stromal cells confirmed the biocompatibility of these fibrous composites. The dual ion release from the bioactive fillers in the PCL matrix is expected to enhance angiogenesis, making the composites relevant for both soft and bone TE.

1. Introduction

Electrospinning (ES) is one of the most used techniques for the fabrication of fibrous materials, being often preferred to solvent casting and phase separation methods because the electrospun fibers possess a higher surface area to volume ratio and high porosity.[1] Moreover, ES is a simple and cost-effective technique that can be applied in almost every field—from biomedical, e.g., drug delivery and tissue engineering (TE) scaffolds,[2,3] to environmental uses, e.g., nanofiber membranes for membrane distillation,[4] and even the production of biological nanosensors[5] and antibacterial filters,[6] thanks to the possibility to fabricate nanostructured fibrous structures starting from different types of polymers, as highlighted in the literature.[7]

The basic principle of the ES process is the application of a high voltage between two electrodes of opposite polarity, a metallic needle containing a polymer solution (or suspension or blend), and a grounded target (collector).[8–10] Because of the application of this electric field, the polymer solution becomes charged, and, as a consequence of the increasing electrostatic

E. Piatti, M. Miola, P. Sartori,[+] E. Verné
Department of Applied Science and Technology (DISAT)
Politecnico di Torino
Corso Duca degli Abruzzi 24, 10129 Turin, Italy
E-mail: enrica.verne@polito.it

The ORCID identification number(s) for the author(s) of this article can be found under https://doi.org/10.1002/adem.202500946.

[+]Present address: Instituto de Nanociencia y Materiales de Aragón, Univestidad de Zaragoza, Zaragoza, Spain

L. Liverani,[++] A. R. Boccaccini
Institute of Biomaterials
Department of Materials Science and Engineering
University of Erlangen-Nürnberg
Cauerstrasse 6, 91058 Erlangen, Germany
E-mail: liliana.liverani@fau.de

[++]Present address: DGS S.p.A., Via Paolo di Dono 73, Rome 00142, Italy

© 2025 The Author(s). Advanced Engineering Materials published by Wiley-VCH GmbH. This is an open access article under the terms of the Creative Commons Attribution License, which permits use, distribution and reproduction in any medium, provided the original work is properly cited.

DOI: 10.1002/adem.202500946

attraction between charges in the polymer solution and the collector, a polymeric fiber jet starts to be ejected from the pendant droplets, initially held at the tip of the syringe by their internal surface tension.[9,11] In detail, when the electrostatic repulsions between charges in the polymer solution reach a critical voltage, exceeding the surface tension of the polymer solution, the droplet changes its shape from a rounded meniscus to a diaphanous and conical protrusion (known as a Taylor cone). The fiber jet travels through the atmosphere in the direction of the external electric field, in two different zones: a first one (called stable zone) in which the jet travels in a direct route and a second zone in which the jet becomes thinner and unstable. During the time of flight, the solvent evaporates from the charged solution and finally solid fibers are collected on the collector.[9]

This technique enables to fabricate micro- and nanofibers which can serve as scaffolds in TE applications, thanks to their similarity with the fibrous structure of the extracellular matrix (ECM). Indeed, according to scaffold-based TE, cells require a 3D biomaterial scaffold that closely mimics the corresponding ECM and acts as a necessary cell guide and supporting template during tissue regeneration.[12] In particular, electrospun scaffolds for soft TE are gaining increasing interest from scientists from all around the globe. The main constituents of soft tissues are collagen fibers and elastin;[13] therefore, biomaterials in the form of fibers are good candidates for the regeneration of these tissues, as shown by many published scientific works[14–20] and related reviews.[21–23]

The term "soft tissues" groups tissues forming blood vessels, skin, muscles, and other organs of our body, except bone.[13] These tissues are complex, fiber-reinforced, and composite structures, characterized by high flexibility and soft mechanical properties.[13] They play a relevant role in our human body, having several organ-specific functions such as protection (skin), transmission of force (ligament and tendons), blood circulation (heart and vessels), and conduction of electrical signals (neurons).[24]

The skin is the largest organ in mammals, encompassing their entire body surface as the first interface with the external environment, serving as protective barrier against potentially harmful mechanical, chemical, and biological stimuli.[25,26] Moreover, it plays a critical role in maintaining the physiological homeostasis of the mammalian body by constant recycling of the basal cell layer.[27] Therefore, a damage to the skin integrity makes the individual susceptible to physiological imbalance, significant disability, or even death.[25]

For the successful regeneration of human tissues, a blood supply is required. Therefore, the formation of new blood vessels (or angiogenesis) is fundamental in TE applications, to ensure an adequate supply of oxygen, essential nutrients, signaling molecules, and growth factors to the injured sites, while removing waste by-products from the surrounding cell environment.[28]

Many materials are available for soft TE applications, including synthetic polymers such as poly-ε(caprolactone) (PCL).[13] Recently, the combination of polymeric materials with bioceramics, such as hydroxyapatite (HA) and bioactive glass (BG) particles, has received increasing attention from researchers working in this field, for the fabrication of soft TE composite scaffolds. However, the experimental research on BG-incorporated polymeric electrospun fibers for soft TE is still limited in comparison to composite electrospun fibers for bone TE.[28] The application of BGs in soft TE has been reviewed by Miguez-Pacheco et al.[29] Kargozar et al.[30,31] and Baino et al.[32] At present, the "healing effect" of BGs on soft tissues is mainly attributed to improved angiogenesis, which is the result of the release of ionic dissolution products from BGs.[31] Many ions, such as copper and boron, have been demonstrated to stimulate angiogenesis and therefore have already been introduced in various BG compositions for soft TE.[33–36] Furthermore, recently, first studies on electrospun polymeric fibers incorporating borate and borosilicate BGs have been carried out.[10,37–39]

In this scenario, the use of the ES technique is particularly interesting, enabling the development of composite fibers containing proangiogenic BGs. However, despite the interesting potential of these composites, achieving a homogeneous dispersion of fillers inside a polymeric fibrous matrix remains a great challenge.

In addition, for optimal tissue regeneration, the problem of infections should not be underestimated. Incorporating antibacterial drugs and/or metallic ions (such as silver[40–42] and copper[43–45]) in engineered composite constructs appears to be a very convenient approach.

Solution parameters (used solvent, polymer concentration, solution viscosity, solution conductivity, and solvent volatility), process parameters (applied electric field, distance needle-collector or working distance, flow rate, needle diameter, and type of collector and needle), and environmental parameters (relative humidity and temperature) affect the ES process and the characteristics of the obtained electrospun materials.[9,28,46] Thus, a careful and time-consuming process optimization is necessary to electrospun fibers with the desired properties for their intended use. In this context, the addition of bioactive fillers plays a relevant role, altering the solution parameters and the final properties of the electrospun composite fibers. Nowadays, the incorporation of substantial amounts of particulate fillers into electrospun fibers is challenging due to their agglomeration inside the ES solution.[47] In fact, micro- or nanosized HA or BG particles tend to form agglomerates in order to reduce the total surface area.[48,49] This leads to difficulties in reaching a uniform dispersion of the particles, leading to reduced ES efficiency and low particle loading capacity, resulting in scaffolds exhibiting poor particle distribution.[47] It is important to notice that the tendency of particles to aggregate increases (and is very high even before the addition to the polymeric solution) by diminishing the particle size.[50,51]

Several attempts have been made in order to prevent filler agglomeration during ES. For example, Kim et al. tried to mix surfactants with the polymer solution before ES.[50] Other authors applied ultrasound (US) energy to the ES solution before ES or by applying the US energy directly to the mixture using an ultrasonic cell disruptor during the ES process.[47,52]

Moreover, it should be underlined that the selection of the appropriate solvent is essential for obtaining smooth, defect-free electrospun fibers. For the fabrication of polymeric electrospun scaffolds, usually harsh toxic solvents such as anhydrous chloroform, dichloromethane, or dimethyl carbonate, dimethylformamide, eventually mixed with ethanol or methanol, are used.[53–56] However, the substitution of such toxic solvents with more environmentally friendly and less harmful solvents (called benign solvents, as defined in[55]) was attempted by many

© 2025 The Author(s). Advanced Engineering Materials published by Wiley-VCH GmbH

15272648, 2025, 4, Downloaded from https://advanced.onlinelibrary.wiley.com/doi/10.1002/adem.202500946, By Marta Miola - Politecnico Di Torino Sist. Bibl Del Polit Di Torino, Wiley Online Library on [12/03/2026]. See the Terms and Conditions (https://onlinelibrary.wiley.com/terms-and-conditions) on Wiley Online Library for rules of use; OA articles are governed by the applicable Creative Commons License

researchers, showing the relevance of the so-called "Green ES" approach.[10,38,39,42,57–63]

In this article, we describe the preparation and characterization of electrospun composite PCL-based fibers incorporating novel sol-gel-derived BG particles doped with B and Cu, for potential use in soft TE. The synthesis of the BGs used in this work has been previously optimized[36] by tailoring the process parameters (such as type, concentration, amount and addition method of the catalyst, and use of centrifugation steps), in order to produce monodispersed spherical submicrometric particles, with very low aggregation and pronounced bioactivity. The ES procedure used to prepare the composite fibers was improved by tuning the process parameters according to the optimized particles and above all by a "green" approach, with particular focus on the use of acetic acid (AA), a benign solvent which belongs to class 3 of solvents according to the guidelines established by the International Conference on Harmonization of Technical Requirements for Registration of Pharmaceuticals for Human Use (ICH).

2. Experimental Section

2.1. Materials

Composite fibers were synthesized using poly(ε-caprolactone) (PCL, 80 kDa, CAS-Number: 24980-41-4, Sigma Aldrich, Munich, Germany) as biopolymer matrix, AA at 98% (AA, CAS Number: 64-19-7, VWR, Germany) as benign solvent for polymer dissolution, and BG particles as bioactive fillers. To synthesize the BG particles, the following reagents were used: tetraorthosilicate (TEOS) $C_8H_{20}O_4Si$ at 99% (Sigma Aldrich), triethyl phosphate (TEP) $C_6H_{15}O_4P$ at 99% (Alfa Aesar), calcium nitrate tetrahydrate $Ca(NO_3)_2{\cdot}4H_2O$, copper nitrate trihydrate $Cu(NO_3)_2{\cdot}3H_2O$ (Fluka), and boric acid H_3BO_3 at 99% (Sigma Aldrich) as source of silica, phosphorus, calcium, copper, and boron oxides, respectively.

2.2. Synthesis of the BG Particles

The synthesis of the BG particles was carried out by an optimized sol-gel synthesis method, focusing on a new BG composition (62% SiO_2-9%P_2O_5-9%CaO-5%CuO-15%B_2O_3), previously designed and developed by Miola et al.[36] as summarized in the flowchart in **Figure 1**. As reported in ref. [36], the synthesis allows to obtain monodispersed spherical particles, with a size range of about 500 nm (evaluated by morphological observations through field-emission scanning electron microscopy (FE-SEM)), a hydrodynamic diameter of 1557 nm, and a polydispersity index of 26.8% (evaluated by DLS analysis[36]).

This new BG was called SBCu, referring S to its silica-based nature, B to the doping with boron, and Cu to the addition of copper in the glass composition.

In order to investigate the effect of boron and copper addition into the glass composition, a 77S glass with the well-known composition 77% SiO_2%–14% CaO–9% P_2O_5 (wt%)[64] was prepared adopting the same synthesis method. This control glass was called S. The different performed synthesis trials and the syntheses of both SBCu and S glasses are more in-depth explained in ref. [36].

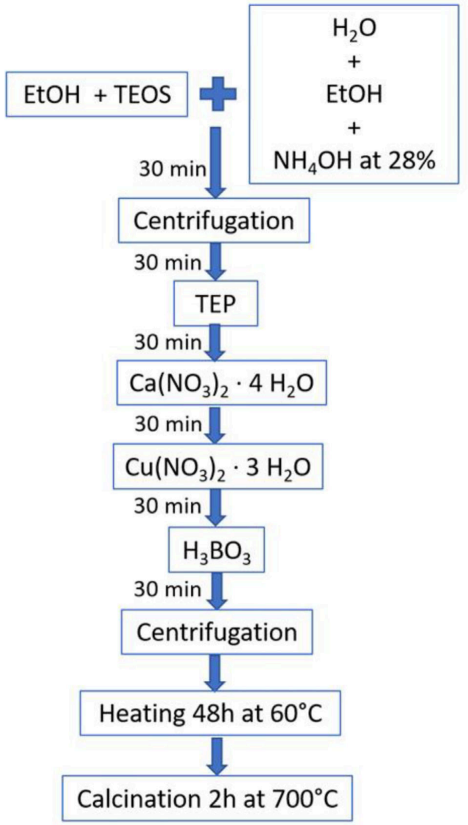


Figure 1. Flowchart of the BG particles preparation steps.

2.3. Synthesis of the Composites

Starting from the approach used in our previous work,[65] the ES process parameters were tailored to improve BG particle dispersion and integration into the PCL matrix. First of all, PCL was dissolved at 20 w/v% in AA, stirring overnight until all PCL grains were dissolved and a clear solution was obtained. To further ensure homogeneity, the polymeric solution was then ultrasonicated for 1 h in an US bath. For the fabrication of composite BG-PCL fibers, BG powders were added to the PCL/AA solution. For this step, various mixing strategies have been proposed in the literature.[38,39,41,42,63,66] In this work, the BG powders were poured into the PCL solution and then manually mixed with a spatula for 1 min, stirred with a magnetic stirrer for 5 min and finally left in a US bath for 2 min.

All ES experiments were performed at room temperature (around 23/24 °C) in air atmosphere with humidity values in

© 2025 The Author(s). Advanced Engineering Materials published by Wiley-VCH GmbH

15272648, 2025, 4, Downloaded from https://advanced.onlinelibrary.wiley.com/doi/10.1002/adem.202500946, By Marta Miola - Politecnico Di Torino Sist. Bibl Del Polit Di Torino, Wiley Online Library on [12/03/2026]. See the Terms and Conditions (https://onlinelibrary.wiley.com/terms-and-conditions) on Wiley Online Library for rules of use; OA articles are governed by the applicable Creative Commons License

the range of 23–26%, by using the horizontal ES setup Starter Kit 40 kV Web (Linari Engineering srl, Valpiana (GR), Italy) and a BD plastic syringe of 3 mL with a cross section of 0.589 cm^2.

Based on previous experimental works,[9,65] the ES process was optimized by changing the following parameters: 1) percentage of BG powders (w/w%) compared to PCL: 20%, 25%, and 30%; 2) flowrate: 0.4, 0.68, 0.82, and 0.96 mL h^{-1}; and 3) diameter of the needle size: 18 and 21 G.

Applied voltage and working distance were kept fixed at 15 kV and 11 cm, respectively, in agreement with previous works of Liverani et al.[9] The spinning time was adjusted in the range of 7–15 min in order to obtain fibrous mats with a suitable comparable thickness.

On the basis of spinning difficulty, size of the electrospun mats, tendency to delaminate during removal of the mat from the collector, and sedimentation of glass particles inside the ES solution, the mats produced with flow rates of 0.68 and 0.82 mL h^{-1} and glass concentrations of 20% and 25% were selected and further characterized.

To evaluate both the influence of glass addition and the effect of the dopant ions boron and copper, control samples were prepared. In particular, neat PCL fibers, without the addition of the glass particles, and composite fibers containing undoped 77S sol-gel control glass particles were synthesized according to previous experimental works.[65] PCL fibers were electrospun for 30 min at 0.4 mL h^{-1}, whereas in the case of 77S-composite fibers (PCL/AA/S), these parameters were identical to the ones used for optimized SBCu-composite fibers. An ES solution with both types of glass and an example of an optimized fibrous mat are shown in **Figure 2**.

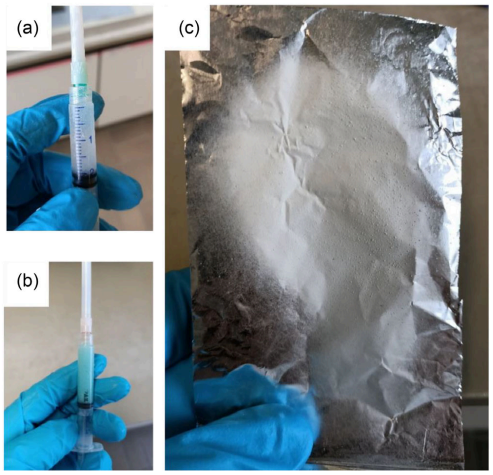


Figure 2. a) ES solution containing S BG (control BG), b) ES solution containing SBCu BG (B- and Cu-doped BG), and c) example of electrospun fibrous mat.

2.4. Characterization

2.4.1. Stability Test

To evaluate whether these new glasses were suitable for the synthesis of composite fibers by using AA as benign solvent for the ES, both S and SBCu glasses were immersed for up to 1 h in AA, according to the ratio used in our previously developed system (PCL/AA) containing B- and Cu doped glasses, as reported in.[65] Thus, 0.4 g of BG powder was immersed in 10 mL of AA. The immersion time was fixed to 1 h, because during our previous experimental works, all composite fibers were produced within 1 h from the preparation of the ES solution containing the BG particles. After 1 h, the glass powders were removed from AA and left to dry under a fume hood. After having removed the acid, bidistilled water was added to wash glass powders and, after a centrifugation at 7000 rpm for 10 min, the liquid was removed, and the glass powders were dried in an incubator at 37 °C. The dried powders were analyzed by scanning electron microscopy (SEM), energy-dispersive X-ray spectroscopy (EDS), X-ray diffraction (XRD).[65] The bioactivity of the AA-treated BGs was also assessed by soaking them in SBF up to 14 days.

2.4.2. Morphological Characterization

Fiber morphology was analyzed by scanning electron microscopy (FE-SEM Auriga, Carl-Zeiss, Germany). Samples were prepared by carefully cutting small sections of the fibers, fixing them on SEM stubs using a carbon tape, and finally sputtering them with gold (Sputter Coater, Q150T, Quorum Technologies) to make them conductive. The diameter of the fibers was estimated from SEM micrographs with the use of the specific tool of the software ImageJ (NIH, USA).[67]

2.4.3. Attenuated Total Reflectance (ATR)-FTIR Analysis

ATR-FTIR spectroscopy was adopted to evaluate the incorporation of the BG nanoparticles inside the polymeric mats. Both neat and composite membranes were characterized using the FTIR spectrometer (Shimadzu IRAffinity-1S, Shimadzu Corp, Japan) in ATR with a selected number of spectral scans of 40, a resolution of 4 cm^{-1}, and a wavenumber range between 4000 and 400 cm^{-1}.

2.4.4. Water Contact Angle (CA) Measurements

The wetting properties of neat and composite fibers were evaluated by water CA measurements on both types of samples, using the CA measurement device Krüss DSA30 (Hamburg, Germany). Prior to carrying out the CA measurements, each sample was fixed on specific 3D printed holders, which were designed with the software Autodesk Inventor (Autodesk, CAL, USA) and printed with Ultimaker S5 3D (**Figure 3**), equipped with the printer software Ultimaker Cura, using a polycarbonate (PC) wire as row material, 260 °C as needle temperature, and 100 °C as plate temperature. By fixing the electrospun mats on these holders, it was possible to keep them well flat.

© 2025 The Author(s). Advanced Engineering Materials published by Wiley-VCH GmbH

15272648, 2025, 4, Downloaded from https://advanced.onlinelibrary.wiley.com/doi/10.1002/adem.202500946, By Marta Miola - Politecnico Di Torino Sist. Bibl Del Polit Di Torino, Wiley Online Library on [12/03/2026]. See the Terms and Conditions (https://onlinelibrary.wiley.com/terms-and-conditions) on Wiley Online Library for rules of use; OA articles are governed by the applicable Creative Commons License

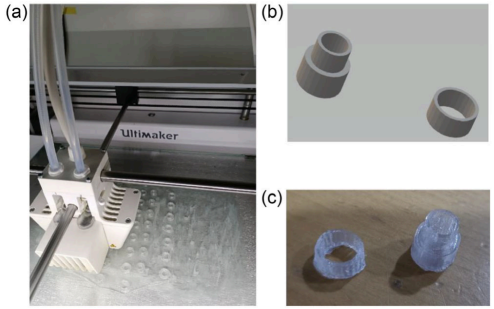


Figure 3. Printing process of the sample holders—a) printer Ultimaker S5 3D printing the holders; b) 3D digital model of the holder; and c) printed holder (inner diameter 4.8 mm).

Measurements were performed in triplicate by dropping 3 µL of distilled water onto different zones of each fibrous mat and then averaging the obtained CA values, which were automatically measured every second in a time frame of 10 s for each tested sample.

2.4.5. Acellular Bioactivity Test

The *in vitro* mineralization ability of the fibers was investigated by immersion in a simulated body fluid (SBF), having ionic concentration similar to the inorganic part of human plasma, prepared following the well-known Kokubo protocol.[68] Portions of fibrous mats were cut and mounted on the same sample holders that were used for the water CA measurements. Then, these samples were soaked in SBF and left in an orbital shaker (KS 4000i control, IKA-Werke GmbH & Co. KG, Germany) at 37 °C for different periods of time (1, 3, 7, and 14 days), never changing the soaking medium. The volume of the needed SBF for each sample was calculated using the same proportion used in the Kokubo protocol, V_S = S_tot/10, where V_S is the volume of the solution (expressed in mL), and S_tot is the sample-medium contact area (expressed in mm^2), which was calculated taking into consideration the inner diameter of the holder (4.8 mm). After each time point, the samples were removed from the SBF, washed with distilled water, dried under fume hood, and characterized through SEM-EDS (Jeol JCH-6000 plus, equipped with EDS device), FTIR, and CA analysis. The pH was monitored during the entire acellular bioactivity test. For each time point and both glasses, the test was done in triplicate for statistical reasons. Empty (without fibers) SBF solution and neat PCL fibers were used as a control. In order to carry out SEM-EDS analysis, the fibrous mats were cut into small pieces, fixed on SEM stubs, and sputtered with chromium.

2.4.6. Mechanical Characterization

In order to study the mechanical properties of the electrospun fibers, a custom-made uniaxial tensile test was carried out at room conditions with a uniaxial testing machine (5960 Dual Column Tabletop Testing System, Instron, Darmstadt, Germany) equipped with a load cell of 100 N at a crosshead speed of 10 mm min^{-1}. As reported in ref. [9], samples were prepared by cutting the electrospun mats in stripes of $3 \times 20\ mm^2$ and then fixing them in a paper frame with inner size of $10 \times 10\ mm^2$ and external size of $20 \times 20\ mm^2$. The thickness of each stripe was measured using a digital micrometer having a precision of 1 µm and then averaging the measured values for better accuracy. In order to obtain a minimum of statistical information, this mechanical test was performed 5 times for each electrospun fibrous mat (PCL/AA, PCL/AA/S, and PCL/AA/SBCu), testing 5 stripes of each mat. The elastic modulus (or Young's modulus) E of the tested samples can be calculated by dividing the applied force (100 N) by the sample area (calculated as $b \times t$ where b is the inner width of the frame, equal to 10 mm, and t is the thickness of the sample stripe).

2.4.7. Cellular Test

In order to assess cell viability and morphology on the electrospun mats, a protocol adapted from a previous work[57] was used.

Bone murine stromal cells ST–2 (Leibniz-Institut DSMZ–German Collection of Microorganisms and Cell Cultures GmbH, Germany) were seeded in RPMI 1640 medium (Thermo Fisher Scientific), supplemented with 10% fetal bovine serum (Lonza) and 1% penicillin/streptomycin (Lonza), and incubated at 37 °C with 5% CO_2, till confluence. The electrospun samples were fixed on holders for a 24-multiwell plate and disinfected with exposure to UV light for 1 h before cell seeding. Drop seeding was performed by using an inoculum ratio of 1.5×10^5 cells mL^{-1} with a drop of 100 µL per sample.

WST-8 assay ((2-(2-methoxy-4-nitrophenyl)- 3-(4-nitrophenyl)-5-(2,4-disulfophenyl)-2H-tetrazolium, monosodium salt), Sigma) was performed 1 and 7 days after the seeding in triplicate on all samples, and results were obtained by using a multiwell plate reader (PHOmo Elisa reader) at 450 nm. More details on the protocol can be found in this article.[57] ANOVA one-way analysis ($p < 0.05$) was performed on the obtained data.

3. Results and Discussion

3.1. Stability of Glass Powders

From EDS results, it was possible to observe that the copper amount slightly decreased after the treatment of SBCu powders with AA, whereas the amounts of the other elements were almost maintained (**Figure 4**a). XRD and FE-SEM analyses on SBCu particles revealed that the formation of HA started from the third day of immersion in SBF (Figure 4c), and after 14 days, well-formed HA crystals were clearly visible on SBCu particles (Figure 4b,d), confirming that the treatment in AA did not compromise the acellular bioactivity of B- and Cu-doped sol-gel glass particles, as previously observed on glass nanoparticles containing B and Cu not treated with AA.[65]

© 2025 The Author(s). Advanced Engineering Materials published by Wiley-VCH GmbH

15272648, 2025, 4, Downloaded from https://advanced.onlinelibrary.wiley.com/doi/10.1002/adem.202500946, By Marta Miola - Politecnico Di Torino Sist. Bibl Del Polit Di Torino, Wiley Online Library on [12/03/2026]. See the Terms and Conditions (https://onlinelibrary.wiley.com/terms-and-conditions) on Wiley Online Library for rules of use; OA articles are governed by the applicable Creative Commons License

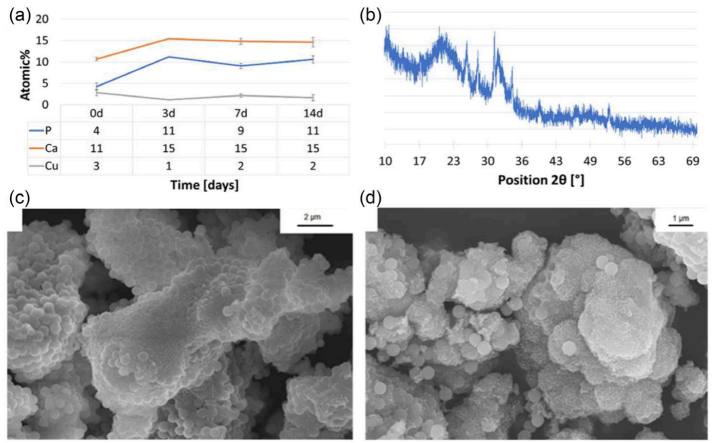


Figure 4. Results of stability test (treatment in AA for 1 h). a) EDS results showing the atomic % of P, Ca, and Cu in SBCu powders after treatment with AA up to 14 days. b) XRD pattern of AA-treated SBCu glass particles after 14 days in SBF. c) SEM micrograph of AA-treated SBCu glass particles after 3 days in SBF (15 K X). d) SEM micrograph of AA-treated glass particles after 14 days in SBF (20 K X).

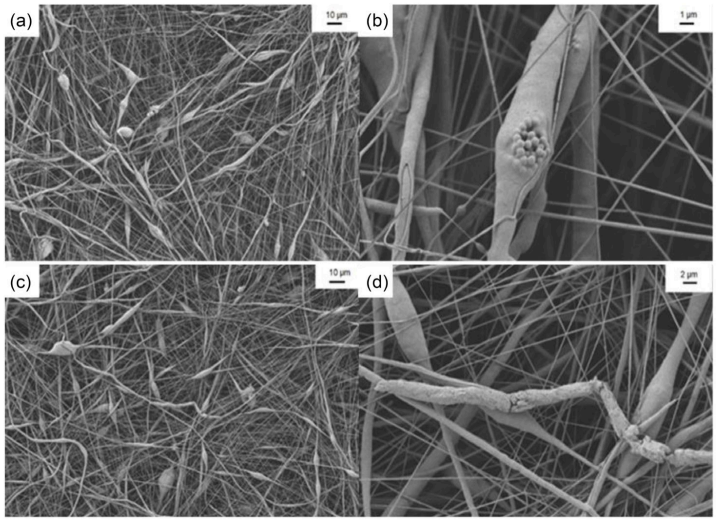


Figure 5. SEM micrograph of PCL/AA/S fibers at a) 1 k and b) 10 k magnifications and PCL/AA/SBCu at c) 1 k and d) 5 k magnifications, obtained with the addition of 20% of BG particles and a flow rate of 0.82 mL h^{-1}.

3.2. Morphological Characterization

Figure 5 shows the morphology of composite fibers containing SBCu glass particles, obtained with a flow rate of 0.82 mL h^{-1} and a glass concentration of 20% (wt/wt). The electrospun fibers show rare defects and are characterized by good particle incorporation inside the fibers. Some BG agglomerates and few fiber shape irregularities are still present (despite the improvement in synthesis) as evidenced in the pictures at higher magnification (Figure 5b,d). However, raising the glass concentration to 25% (wt/wt) or fixing the flow rate at 0.68 mL h^{-1}, even more defects, beads, and irregularities in

© 2025 The Author(s). Advanced Engineering Materials published by Wiley-VCH GmbH

15272648, 2025, 4, Downloaded from https://advanced.onlinelibrary.wiley.com/doi/10.1002/adem.202500946, By Marta Miola - Politecnico Di Torino Sist. Bibl Del Polit Di Torino, Wiley Online Library on [12/03/2026]. See the Terms and Conditions (https://onlinelibrary.wiley.com/terms-and-conditions) on Wiley Online Library for rules of use; OA articles are governed by the applicable Creative Commons License

the shape and dimensions of the fibers were observed (data not shown). Therefore, a flow rate of 0.82 mL h^{-1} and a glass concentration of 20% (wt/wt) were chosen as the best parameters for ES of the B- and Cu-doped composite fibers. Thus, in the following paragraphs, the SBCu-fibers electrospun with the selected parameters will be simply named PCL/AA/SBCu and compared with control S-fibers electrospun in the same conditions, labelled PCL/AA/S.

The diameter of the selected fibers was then determined from SEM micrographs using the software ImageJ, calculating the diameter of 25 fibers and averaging the measured values. In comparison with the previous literature results of Liverani et al.[9] on neat PCL fibers produced using the same reagents, polymer concentration, and ES parameters, on which an average diameter of 1.0 ± 0.1 µm has been detected, in the present experimental work, a decrease in average diameter of composite fibers, even of one half, was observed. We hypothesized that the reduction in fiber diameter might be partly attributed to the release of cationic species from BGs' surface, leading to increased conductivity. The greater number of charges carried by the jet imposes higher elongation forces, resulting in thinner fibers, as reported in ref. [59].

3.3. ATR-FTIR Analysis

The FTIR analysis on both the neat PCL and composite fibers (data not shown) did not differ one each other, showing just the main absorption bands of PCL, i.e., asymmetric and symmetric CH_2 stretching (2943 and 2866 cm^{-1}), carbonyl (C═O) stretching peak (1722 cm^{-1}), C─C stretching peak (1294 cm^{-1}), and asymmetric and symmetric C─O─C stretching peaks (1240 and 1165 cm^{-1}).[9,69] Coherently with previous works,[19] the absorption bands that could be linked with the presence of BGs inside the PCL matrix were not detected, being almost completely masked by the bands of PCL itself. Just a small increase in peak at 1085 cm^{-1} and a weak peak at 464 cm^{-1} were visible, which could be associated with the absorption bands of the asymmetric stretching mode[19,20,70,71] and rocking vibration[20,71] of Si─O─Si in silicates, but their intensities are too low to be clearly attributed to the BG particles.

3.4. Water CA Measurements

The inclusion of BGs in polymeric hydrophobic fibrous materials increased their hydrophilicity and wettability, if compared with neat PCL mats. This increase was not substantial, being the CA of the composites still slightly higher than 90° (threshold value between the hydrophilic and hydrophobic behaviors of a surface) and equal to $93.4° \pm 4$ and $97.5° \pm 3$ for PCL/AA/S and PCL/AA/SBCu, respectively. These results are shown in **Figure 6** as mean values of three CA measurements. In comparison with our previous work,[65] a pronounced difference can be evidenced for both the CA results and their standard deviations. In ref. [65], the composite fibers showed a hydrophobic behavior, not so different from neat PCL. This was explained considering that the glass particles were smaller than 100 nm, forming micrometer-scale aggregates not homogeneously dispersed in the PCL matrix; the presence of clusters and the related enhanced roughness of the fiber surface have been correlated with this behavior. The samples described in the present work have been improved in terms of BG size, aggregation, and dispersion, achieving better wettability, although not yet optimal, compared to what was described in ref. [36]. Their not completely hydrophilic behavior, although significantly improved, can also be explained in this case by referring to the residual tendency of the BG particles to aggregate and the consequent slight surface roughness that can arise, similarly to what was more massively observed in ref. [65]. This is consistent with the Wenzel model, which explains how roughness modifies the wettability characteristics, depending on the nature of the surface.[72] In particular, the surface roughness conferred by the agglomeration of the glass

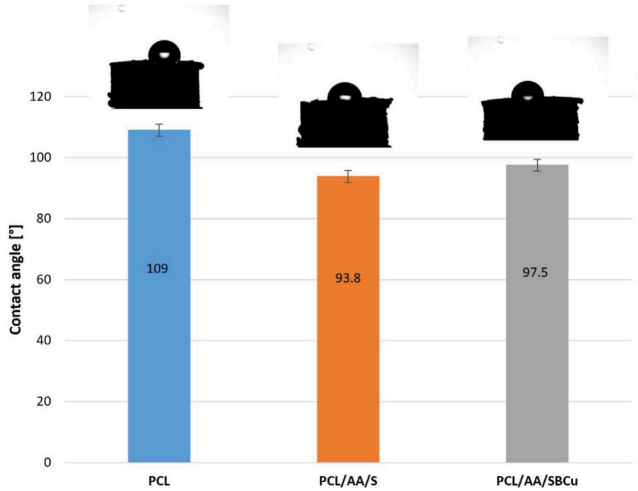


Figure 6. Results of CA measurements performed on neat (PCL) and composite fibers (PCL/AA/S and PCL/AA/SBCu).

© 2025 The Author(s). Advanced Engineering Materials published by Wiley-VCH GmbH

15272648, 2025, 4, Downloaded from https://advanced.onlinelibrary.wiley.com/doi/10.1002/adem.202500946, By Marta Miola - Politecnico Di Torino Sist. Bibl Del Polit Di Torino, Wiley Online Library on [12/03/2026]. See the Terms and Conditions (https://onlinelibrary.wiley.com/terms-and-conditions) on Wiley Online Library for rules of use; OA articles are governed by the applicable Creative Commons License

particles increases the surface hydrophobicity of the investigated fibers, which already have a hydrophobic surface at the outset.

3.5. Acellular Bioactivity Test

During the acellular bioactivity test, the pH trends of both composite fibers (with SBCu and with control glass S) were almost linear, very slightly increasing up to 7.60 and 7.64 for PCL/AA/S and PCL/AA/SBCu (respectively) after 14 days in SBF (**Figure 7**). This result could be related to the buffering effect of boron, in agreement with literature.[36,73] In fact, during the bioactivity test of almost any BG composition, the pH of SBF gradually increases, due to the ionic exchange that occurs between BGs' surface Ca^{2+} ions and H^+ ions from the SBF, inducing a depletion of H^+ ions in the solution. It is also well known that pH values reached by the SBF depend on the BG composition. B-containing glasses usually show a flatter trend in pH values and, in general, lower pH values if compared to other BGs not containing boron. This behavior is often related to the mild acidification effect derived from the B-containing BGs surface dissolution, because of the hydrolysis of boron oxide leading to the formation of boron acid derivatives, which, in turn,

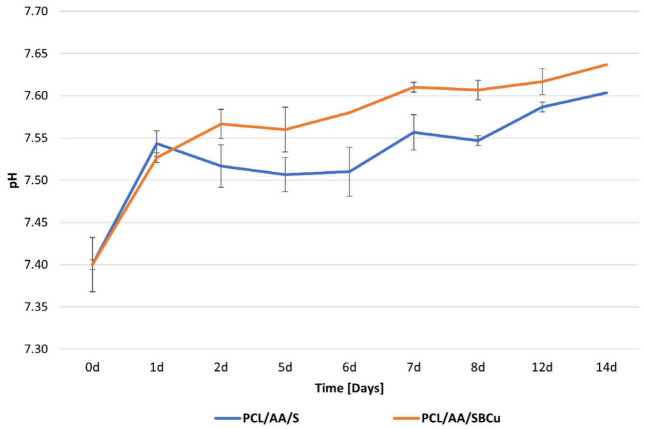


Figure 7. pH trend of the SBF solution where PCL/AA/S and PCL/AA/SBCu were immersed during acellular bioactivity test.

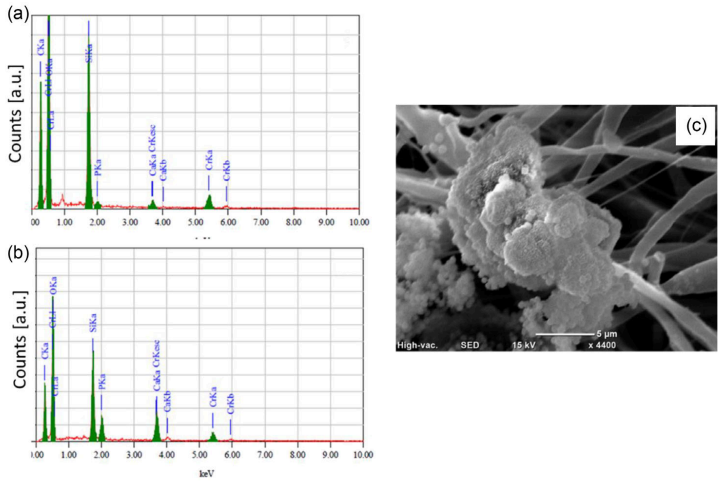


Figure 8. EDS pattern of PCL/AA/SBCu a) after 1 day and b) after 14 days in SBF. c) SEM micrograph of PCL/AA/SBCu after 14 days in SBF, showing deposited HA crystals.

© 2025 The Author(s). Advanced Engineering Materials published by Wiley-VCH GmbH

15272648, 2025, 4, Downloaded from https://advanced.onlinelibrary.wiley.com/doi/10.1002/adem.202500946, By Marta Miola - Politecnico Di Torino Sist. Bibl Del Polit Di Torino, Wiley Online Library on [12/03/2026]. See the Terms and Conditions (https://onlinelibrary.wiley.com/terms-and-conditions) on Wiley Online Library for rules of use; OA articles are governed by the applicable Creative Commons License

partially compensates the pH increase due to the depletion of H^+ ions. Since cultured human cells are sensitive to extracellular pH *in vitro*, the "buffering" capacity of the B-glass containing composite mats may be relevant for *in vitro* studies. According to good laboratory practice, maintaining the pH of cell cultures between 7.2 and 7.4 is essential, as significant deviations can affect cell membrane function. Therefore, substantial local pH alterations caused by burst ion release could lead to pH-dependent cytotoxic effects.[74]

EDS analyses after 1 and 14 days of SBF immersion are reported in **Figure 8**a,b. After 1 day of immersion, no substantial changes in composition are observed; Ca and P begin to increase slightly after 3 days (data not reported) and undergo a significant increase at 14 days. From SEM analyses, few crystals of HA were observed for the first time on the surface of the composite mats after 7 days in SBF, evolving to more defined globular aggregates after 14 days of immersion in SBF (Figure 8c).

The bioactivity of both composite fibers was also confirmed by FTIR analysis by comparing FTIR spectra of the electrospun composite fibers before and after immersion in SBF. In addition to the PCL peaks described in paragraph 3.3, it is possible to observe the presence of new peaks emerging after immersion: 1) peak around 3180 cm^{-1}, probably related to changes in the structure of the OH groups from Si—OH to Si—O—Na^+ bonds,[75] 2) small peak around 1664 cm^{-1}, attributable to the presence of carbonated apatite or even pure apatite,[76] 3) peak at around 1550 cm^{-1} due to Ca^{2+} coordinated CO_3^{2-} adsorption or carbonate ions substituted in carbonated apatites,[77] and 4) small double peak around 660–643 cm^{-1}, associated with the formation of HA.[75]

All other peaks that could be eventually linked to the mineralization of these composites were masked by PCL peaks and could not be recognized. In **Figure 9**, FTIR spectra of fibers immersed up to 14 days are reported, stressing the presence of the above-mentioned peaks related to HA.

Finally, in order to evaluate wettability variation during the immersion in SBF, water CA measurements were performed after immersion in SBF. This analysis showed (**Figure 10**) that the CA of both PCL/AA/SBCu and control PCL/AA/S decreased during immersion in SBF, since the first time point (1 day), at which both composite fibers showed higher wettability and hydrophilicity (56.6° for PCL/AA/S and 73.77° for PCL/AA/

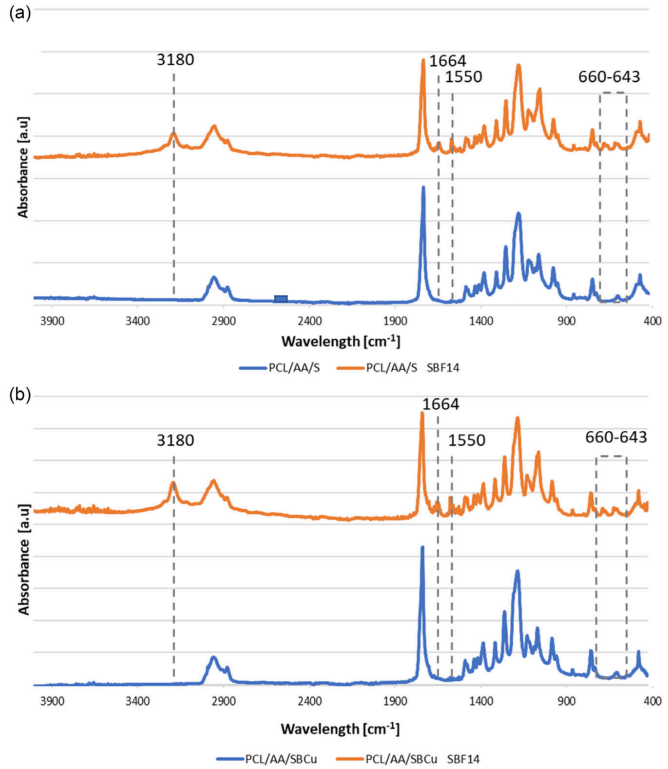


Figure 9. a) FTIR spectra of PCL/AA/S and b) PCL/AA/SBCu before and after 14 days of immersion in SBF.

© 2025 The Author(s). Advanced Engineering Materials published by Wiley-VCH GmbH

15272648, 2025, 4, Downloaded from https://advanced.onlinelibrary.wiley.com/doi/10.1002/adem.202500946, By Marta Miola - Politecnico Di Torino Sist. Bibl Del Polit Di Torino, Wiley Online Library on [12/03/2026]. See the Terms and Conditions (https://onlinelibrary.wiley.com/terms-and-conditions) on Wiley Online Library for rules of use; OA articles are governed by the applicable Creative Commons License

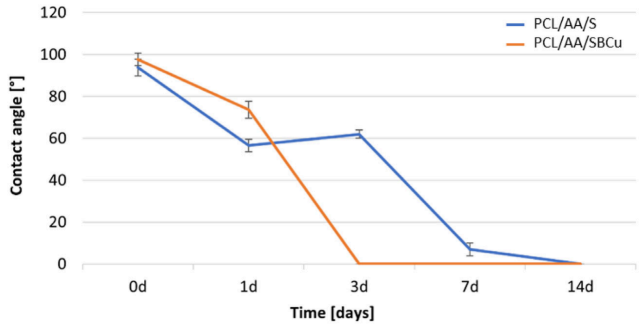


Figure 10. Results of CA measurements on PCL/AA/SBCu and PCL/AA/S samples after immersion in SBF up to 14 days.

SBCu) if compared to neat PCL and composite fibers before the immersion in SBF (see Figure 6 for comparison). However, it should also be observed that the water CA is not only a measure of hydrophilic properties but also of the porosity of the material, which could be increased during the acellular bioactivity.

Therefore, on the basis of these results, it is possible to conclude that the bioactivity of the composites was enhanced thanks to the incorporation of the optimized BG particles S and SBCu, if compared to previous results.[19,39,78] Indeed, Lepry et al. have observed the formation of HA after 7 days in SBF,[39] whereas Moura et al.[19] have observed it only after 21 days. In addition, in a previous work of Liverani et al.[78] no HA formation was observed because of the detachment of the BG particles from the polymer matrix after only 1 day of immersion.

3.6. Mechanical Characterization

A relevant problem and recurring failure cause of implants is the mismatch between the graft and the host tissue.[79] Therefore, it is crucial to evaluate the mechanical properties of the composite fiber, reported in terms of average and standard deviation (±SD) in **Table 1**.

As expected for electrospun polymer-based fibers and in agreement with literature results and our previous experimental works, both neat polymeric and composite fibers showed a stress-strain curve (not reported) characterized by a first linear elastic trend (Hookean response) and a second nonlinear trend (plastic behavior related to the fiber alignment before the sample fracture).[78,80] As reported in Table 1, the synthesized composite fibers showed Young's modulus averaged values lower than that of neat PCL fibers, even if, according to scientific literature, the addition of an inorganic filler usually increases the Young's modulus of polymers.[52,81]

Table 1. Mechanical properties of both neat and composite fibers.

Sample	Tensile strain at break [%]	UTS [MPa]	E [MPa]
PCL/AA	255 ± 38	4 ± 1	33 ± 7
PCL/AA/S	138 ± 18	2.4 ± 0.4	9 ± 2
PCL/AA/SBCu	240 ± 26	2 ± 1	10 ± 5

Moreover, as a consequence of the addition of glass particles inside the polymeric matrix, also the ultimate tensile strength (UTS) was slightly decreased. However, this decrease was comparable with literature results.[19,82] A small enhancement in comparison to our previous experimental work on fibers containing similar glass particles[64] should be pointed out, as a consequence of the synthesis optimization.

Regarding the measured reduction of the tensile strain, it is well known that the introduction of a rigid phase, such as BG particles, in a polymeric soft matrix limits its plastic deformation and elongation.[19,53,54,83,84]

The results (in particular the low values of E and UTS) could be influenced by the not-completely homogeneous distribution of the BG fillers inside the fibers, which could lower the mechanical properties of the material, leading to nonuniform variation in the fiber diameter, presence of surface roughness and formation of a weak points/defects in the material that caused cracks and enhanced catastrophic failure, in agreement with previous experimental results.[9,19,47,81,82,85] In fact, standard deviation values are not negligible, indicating a high dispersion of the measured values. It is worth noticing that the achievement of a well-dispersed particle distribution inside composite fibrous mats is still an important open issue in the field of electrospun scaffolds.[86]

Considering these observations, the composite electrospun mats developed in this project could be potential candidates for soft TE applications, being their mechanical properties in the required range ($E = 0.4$–350 MPa, UTS = 2–12 MPa).

3.7. Cell Viability

The stromal cell line ST-2, derived from mouse bone marrow, was selected because it showed osteoblast,[87,88] chondrocyte,[89] and adipocyte differentiation,[90,91] confirming to be a suitable cell line for preliminary assessment (cell viability and proliferation) for both soft and hard TE applications. As reported in **Figure 11**, according to one-way ANOVA ($p < 0.05$), cell adhesion and viability on the composite electrospun fibers, 1 day after seeding, were comparable with the neat PCL/AA ones. However, although the

 © 2025 The Author(s). Advanced Engineering Materials published by Wiley-VCH GmbH

15272648, 2025, 4, Downloaded from https://advanced.onlinelibrary.wiley.com/doi/10.1002/adem.202500946, By Marta Miola - Politecnico Di Torino Sist. Bibl Del Polit Di Torino, Wiley Online Library on [12/03/2026]. See the Terms and Conditions (https://onlinelibrary.wiley.com/terms-and-conditions) on Wiley Online Library for rules of use; OA articles are governed by the applicable Creative Commons License

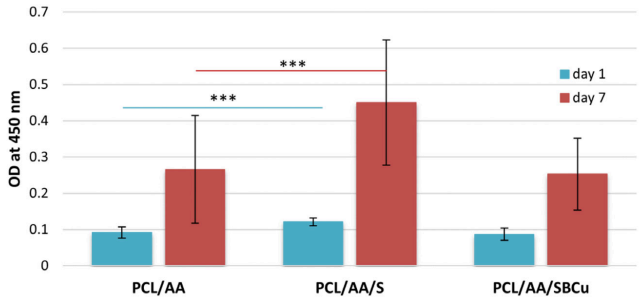


Figure 11. WST-8 analysis: histograms of OD at 450 nm for all samples (PCL/AA, PCL/AA/S, and PCL/AA/SBCu) after 1 and 7 days of cell seeding.

OD values (at 450 nm) for PCL/AA/SBCu did not show significant differences from those of the neat PCL/AA, the OD values for PCL/AA/S were slightly higher than the neat PCL/AA in a statistically significant way. Analogously, 7 days after the seeding, the OD values for PCL/AA/SBCu were comparable with those of neat PCL/AA fibers, and in the case of PCL/AA/S, the increase in OD values was statistically significant in comparison to neat PCL/AA. It is worth of mentioning that the increase in the absorbance measured 7 days after the seeding was relevant for all the samples (composites and control ones), confirming that the inclusion of the glass particles did not inhibit cell proliferation, even in the presence of B and Cu as dopant elements. This result is consistent with the properties of BGs, which, on one hand, are well known to facilitate the proliferation of progenitor cells of soft and calcified tissues but on the other hand may cause a few decrease in cell adhesion, due to the ion release phenomena and to the increase in pH, intrinsic of the bioactivity mechanism. This phenomenon can be considered quite relevant in the case of the PCL/AA/SBCu composites, which indeed produce a slight increase in pH compared to PCL/AA/S (Figure 7). Such results are in line with our previous work, concerning composites incorporating B- and Cu-doped BG aggregated particles.[6]

4. Conclusions

The aim of this study was the synthesis optimization of electrospun composite PCL-based fibers incorporating spherical sol-gel-derived BG particles doped with B and Cu, for potential use in soft TE. The BG particles were synthesized through a sol-gel procedure, which allowed to obtain monodisperse particles exhibiting a round shape and a low aggregation state. The ES procedure was carried out using benign solvents. After a careful optimization of the process parameters, new composite fibrous mats containing B- and Cu-doped BG particles and showing satisfying properties were successfully prepared. Due to the good retention of the BG particles inside the PCL matrix, the composite fibers showed excellent bioactive behavior, as evidenced by the presence of FTIR peaks related to HA starting from the first day of immersion in SBF and the deposition of mature HA crystals on the fiber surface already after 7 days of immersion. Although the glass particles appeared still noncompletely homogeneously dispersed into the fibers, the results obtained by wettability, mechanical and cytocompatibility tests were considered adequate for the potential use of these composites for soft TE applications.

Acknowledgements

Open access publishing facilitated by Politecnico di Torino, as part of the Wiley - CRUI-CARE agreement.

Conflict of Interest

The authors declare no conflict of interest.

Data Availability Statement

The data that support the findings of this study are available from the corresponding author upon reasonable request.

Keywords

benign solvents, bioactive glass, boron, composite, copper, electrospinning, poly(ε-caprolactone)

Received: April 7, 2025
Revised: October 7, 2025
Published online: November 9, 2025

[1] A. Haider, S. Haider, I. K. Kang, *Arabian J. Chem.* **2018**, *11*, 1165.
[2] R. Sridhar, S. Sundarrajan, J. R. Venugopal, R. Ravichandran, S. Ramakrishna, *J. Biomater. Sci., Polym. Ed.* **2013**, *24*, 365.
[3] X. Hu, S. Liu, G. Zhou, Y. Huang, Z. Xie, X. Jing, *J. Controlled Release* **2014**, *185*, 12.
[4] C. Feng, K. C. Khulbe, T. Matsuura, S. Tabe, A. F. Ismail, *Sep. Purif. Technol.* **2013**, *102*, 118.
[5] Z. M. Huang, Y. Z. Zhang, M. Kotaki, S. Ramakrishna, *Compos. Sci. Technol.* **2003**, *63*, 2223.
[6] H. Ma, B. S. Hsiao, B. Chu, *J. Memb. Sci.* **2014**, *452*, 446.
[7] J. D. Schiffman, C. L. Schauer, *Polym. Rev.* **2008**, *48*, 317.
[8] N. Bhardwaj, S. C. Kundu, *Biotechnol. Adv.* **2010**, *28*, 325.
[9] L. Liverani, A. R. Boccaccini, *Nanomaterials* **2016**, *6*, 75.

 © 2025 The Author(s). Advanced Engineering Materials published by Wiley-VCH GmbH

15272648, 2025, 4, Downloaded from https://advanced.onlinelibrary.wiley.com/doi/10.1002/adem.202500946, By Marta Miola - Politecnico Di Torino Sist. Bibl Del Polit Di Torino, Wiley Online Library on [12/03/2026]. See the Terms and Conditions (https://onlinelibrary.wiley.com/terms-and-conditions) on Wiley Online Library for rules of use; OA articles are governed by the applicable Creative Commons License

[10] M. Luginina, K. Schuhladen, R. Orrú, G. Cao, A. R. Boccaccini, L. Liverani, *Nanomaterials* **2020**, *10*, 1.
[11] K. C. Lim, *Prog. Polym. Sci.* **2017**, *70*, 1.
[12] T. Billiet, M. Vandenhaute, J. Schelfhout, S. Van Vlierberghe, P. Dubruel, *Biomaterials* **2012**, *33*, 6020.
[13] L. C. du Toit, P. Kumar, Y. E. Choonara, V. Pillay, *Nanobiomater.: Nanostruct. Mater. Biomed. Appl.* **2018**, 257.
[14] O. Bas, S. Lucarotti, D. D. Angella, N. J. Castro, C. Meinert, F. M. Wunner, E. Rank, G. Vozzi, T. J. Klein, I. Catelas, E. M. De-Juan-Pardo, D. W. Hutmacher et al., *Chem. Eng. J.* **2018**, *340*, 15.
[15] B. Pei, W. Wang, Y. Fan, X. Wang, F. Watari, X. Li, *Regen. Biomater.* **2017**, *4*, 257.
[16] N. M. Lee, C. Erisken, T. Iskratsch, M. Sheetz, W. N. Levine, H. H. Lu, *Biomaterials* **2017**, *112*, 303.
[17] L. Liverani, A. Piegat, A. Niemczyk, M. El Fray, A. R. Boccaccini, *Eur. Polym. J.* **2016**, *81*, 295.
[18] D. Moura, M. T. Souza, L. Liverani, G. Rella, G. M. Luz, J. F. Mano, A. R. Boccaccini, *Mater. Sci. Eng., C* **2017**, *76*, 224.
[19] R. B. Trinca, C. B. Westin, J. A. F. da Silva, Â. M. Moraes, *Eur. Polym. J.* **2017**, *88*, 161.
[20] A. Motameni, I. S. Çardaklı, R. Gürbüz, A. Z. Alshemary, M. Razavi, O. M. C. Farukoğlu, *Int. J. Polym. Mater.* **2024**, *73*, 600.
[21] M. C. Araque-Monrós, D. M. García-Cruz, J. L. Escobar-Ivirico, L. Gil-Santos, M. Monleón-Pradas, J. Más-Estellés, *Ann. Biomed. Eng.* **2020**, *48*, 757.
[22] M. Zhang, S. Xu, R. Wang, Y. Che, C. Han, W. Feng, C. Wang, W. Zhao, *J. Mater. Sci. Technol.* **2023**, *162*, 157.
[23] J. Wang, M. Windbergs, *Eur. J. Pharm. Biopharm.* **2017**, *119*, 283.
[24] J. Nam, N. Won, J. Bang, H. Jin, J. Park, S. Jung, S. Jung, Y. Park, S. Kim, *Adv. Drug Deliv. Rev.* **2013**, *65*, 536.
[25] X. Wang, J. Chang, C. Wu, *Appl. Mater. Today* **2018**, *11*, 308.
[26] D. J. Tobina, *Chem. Soc. Rev.* **2006**, *35*, 52.
[27] A. D. Metcalfe, M. W. J. Ferguson, *Biomaterials* **2007**, *28*, 5100.
[28] S. Nazarnezhad, F. Baino, H. W. Kim, T. J. Webster, S. Kargozar, *Nanomaterials* **2020**, *10*, 1.
[29] V. Miguez-Pacheco, L. L. Hench, A. R. Boccaccini, *Acta Biomater.* **2015**, *13*, 1.
[30] S. Kargozar, S. Hamzehlou, F. Baino, *Materials* **2017**, *10*, 1.
[31] S. Kargozar, F. Baino, S. Hamzehlou, R. G. Hill, M. Mozafari, *Trends Biotechnol.* **2018**, *36*, 430.
[32] F. Baino, H. Sepideh, S. Kargozar, *J. Funct. Biomater.* **2018**, *9*, 1.
[33] Q. Yang, S. Chen, H. Shi, H. Xiao, Y. Ma, *Mater. Sci. Eng., C* **2015**, *55*, 105.
[34] C. Stähli, M. James-Bhasin, A. Hoppe, A. R. Boccaccini, S. N. Nazhat, *Acta Biomater.* **2015**, *19*, 15.
[35] J. Zhou, H. Wang, S. Zhao, N. Zhou, L. Li, W. Huang, D. Wang, C. Zhang, *Mater. Sci. Eng., C* **2016**, *60*, 437.
[36] M. Miola, E. Piatti, P. Sartori, E. Vernè, *J. Non-Cryst. Solids* **2023**, *622*, 122653.
[37] J. S Fernandes, P. Gentile, M. Martins, N. M Neves, C. Miller, A. Crawford, R. A Pires, P. Hatton, R. L Reis, *Acta Biomater.* **2016**, *44*, 168.
[38] S. Chen, M. Michálek, D. Galusková, M. Michálková, P. Švančárek, A. Talimian, H. Kaňková, J. Kraxner, K. Zheng, L. Liverani, D. Galusek, A. R. Boccaccini, *Materials Science and Engineering: C.* **2020**, *112*, 110909.
[39] O. Access, W. C. Lepry, S. Smith, L. Liverani, A. R. Boccaccini, S. N. Nazhat, *Biomed. Glasses* **2016**, *2*, 88.
[40] A. Hu, J. Zhou, *Adv. NanoBiomed Res.* **2025**, *5*, 2500004.
[41] M. Miola, G. Fucale, G. Maina, E. Verné, *Biomed. Mater.* **2015**, *10*, 55014.
[42] F. E. Ciraldo, L. Liverani, L. Gritsch, W. H. Goldmann, A. R. Boccaccini, *Materials* **2018**, *11*, 1.
[43] Q. Shen, Y. Qi, Y. Kong, H. Bao, Y. Wang, A. Dong, H. Wu, Y. Xu, *Front Bioeng. Biotechnol.* **2022**, *20*, 795425.
[44] M. Miola, E. Verné, *Materials* **2016**, *9*, 1.
[45] S. Chitra, P. Bargavi, M. Balasubramaniam, R. R. Chandran, S. Balakumar, *Mater. Sci. Eng., C* **2020**, *109*, 110598.
[46] V. Perez-Puyana, M. Jiménez-Rosado, A. Romero, A. Guerrero, *Polymers* **2020**, *12*, 1.
[47] H. W. Tong, M. Wang, Z. Y. Li, W. W. Lu, *Biomed. Mater.* **2010**, *5*, 054111.
[48] L. Grøndahl, K. Jack, *Biomed. Compos.* **2009**, *101*, 83.
[49] F. Álvarez-Carrasco, P. Varela, M. A. Sarabia-Vallejos, C. García-Herrera, M. Saavedra, P. A. Zapata, D. Zárate-Triviño, J. J. Martínez, D. A. Canales, *Int. J. Mol. Sci.* **2024**, *25*, 6843.
[50] C. Vichery, J.-M. Nedelec, *Materials* **2016**, *9*, 1.
[51] H. W. Kim, H. H. Lee, J. C. Knowles, *J. Biomed. Mater. Res. A* **2006**, *79*, 643.
[52] E. Bahremandi Toloue, M. Mohammadalipour, S. Mukherjee, S. Karbasi, *Int. J. Biol. Macromol.* **2024**, *254*, 12786.
[53] M. Kouhi, M. Morshed, J. Varshosaz, M. H. Fathi, *Chem. Eng. J.* **2013**, *228*, 1057.
[54] M. S. Kang, J. H. Kim, R. K. Singh, J. H. Jang, H. W. Kim, *Acta Biomater.* **2015**, *16*, 103.
[55] M. Putti, M. Simonet, R. Solberg, G. W. M. Peters, *Polymer* **2015**, *63*, 189.
[56] L. H. Pitaluga, M. T. Souza, E. D. Zanotto, M. E. S. Romero, P. V. Hatton, *Materials* **2018**, *11*.
[57] L. Liverani, M. S. Killian, A. R. Boccaccini, *Front. Bioeng. Biotechnol.* **2019**, *7*, 1.
[58] M. J. Mochane, T. S. Motsoeneng, E. R. Sadiku, T. C. Mokhena, J. S. Sefadi, *Appl. Sci.* **2019**, *9*, 1.
[59] L. Van Der Schueren, I. Steyaert, B. De Schoenmaker, K. De Clerck, *Carbohydr. Polym.* **2012**, *88*, 1221.
[60] K. Ghosal, S. Thomas, N. Kalarikkal, A. Gnanamani, *J. Polym. Res.* **2014**, *21*, 2.
[61] D. Dippold, A. Cai, M. Hardt, A. R. Boccaccini, R. Horch, J. P. Beier, D. W. Schubert, *Mater. Sci. Eng., C* **2017**, *72*, 278.
[62] J. Dulnik, D. Kołbuk, P. Denis, P. Sajkiewicz, *Eur. Polym. J.* **2018**, *104*, 147.
[63] L. Liverani, J. Lacina, J. A. Roether, E. Boccardi, M. S. Killian, P. Schmuki, D. W. Schubert, A. R. Boccaccini, *Bioact. Mater.* **2018**, *3*, 55.
[64] V. Aina, Fr. Bonino, C. Morterra, M. Miola, C. L. Bianchi, Gi. Malavasi, M. Marchetti, V. Bolis, *J. Phys. Chem.* **2011**, *115*, 2196.
[65] E. Piatti, M. Miola, L. Liverani, E. Verné, A. R. Boccaccini, *J. Biomed. Mater. Res. A* **2023**, *111*, 1692.
[66] F. Serio, M. Miola, E. Verné, D. Pisignano, A. R. Boccaccini, L. Liverani, *Nanomaterials* **2019**, *9*, 1.
[67] C. A. Schneider, W. S. Rasband, K. W. Eliceiri, *Nat. Methods* **2012**, *9*, 671.
[68] K. Tadashi, H. Takadama, T. Kokubo, H. Takadama, K. Tadashi, H. Takadama, *Biomaterials* **2006**, *27*, 2907.
[69] M. Li, M. J. Mondrinos, X. Chen, M. R. Gandhi, F. K. Ko, P. I. Lelkes, *J. Biomed. Mater. Res. A* **2006**, *79*, 963.
[70] Q. Chen, G. A. Thouas, *Acta Biomater.* **2011**, *7*, 3616.
[71] G. M. Luz, J. F. Mano, *Nanotechnology* **2011**, *22*, 1.
[72] S. Azizian, M. Khosravi, in *Interface Science and Technology, Volume 30: Advanced Low-Cost Separation Techniques*, Chapter 12, (Eds: G. Z. Kyzas, C. Athanasios) Mitropoulos - Hephaestus Advanced Laboratory, Department of Chemistry, International Hellenic University, Kavala, Greece **2019**, pp. 283–332.
[73] R. M. Radn, A. Z. Alshemary, Z. Evis, D. Keskin, K. Altunbaş, A. Tezcaner, *Ceram Int.* **2018**, *44*, 9854.

 © 2025 The Author(s). Advanced Engineering Materials published by Wiley-VCH GmbH

15272648, 2025, 4, Downloaded from https://advanced.onlinelibrary.wiley.com/doi/10.1002/adem.202500946, By Marta Miola - Politecnico Di Torino Sist. Bibl Del Polit Di Torino, Wiley Online Library on [12/03/2026]. See the Terms and Conditions (https://onlinelibrary.wiley.com/terms-and-conditions) on Wiley Online Library for rules of use; OA articles are governed by the applicable Creative Commons License

[74] F. E. Ciraldo, E. Boccardi, V. Melli, F. Westhauser, A. R. Boccaccini, *Acta Biomat.* **2018**, *75*, 3.
[75] R. G. Furlan, W. R. Correr, A. F. C. Russi, M. R. da Costa Iemma, E. Trovatti, É. Pecoraro, *J. Sol-Gel Sci. Technol.* **2018**, *88*, 181.
[76] M. Mozafari, F. Moztarzadeh, M. Tahriri, *J. Non Cryst. Solids* **2010**, *356*, 1470.
[77] M. Mac˘kovic´, A. Hoppe, R. Detsch, D. Mohn, W. J. Stark, E. Spiecker, A. R. Boccaccini, *J. Nanopart. Res.* **2012**, *14*, 966.
[78] L. Liverani, E. Boccardi, A. M. Beltrán, A. R. Boccaccini, *Polymers* **2017**, *9*, 1.
[79] S. Ramakrishna, J. Mayer, E. Wintermantel, K. W. Leong, *Compos. Sci. Technol.* **2001**, *61*, 1189.
[80] J. Dulnik, P. Denis, P. Sajkiewicz, D. Kołbuk, B. Choinska, *Polym. Degrad. Stab.* **2016**, *130*, 10.
[81] J. H. Jo, E. J. Lee, D. S. Shin, H. E. Kim, H. W. Kim, Y. H. Koh, J. H. Jang et al., *J. Biomed. Mater. Res. Part B* **2009**, *91*, 213.
[82] N. C. Bleach, S. N. Nazhat, K. E. Tanner, M. Kellomäki, P. Törmälä, *Biomaterials* **2002**, *23*, 1579.
[83] M. Otadi, D. Mohebbi-Kalhori, *Procedia Mater. Sci.* **2015**, *11*, 196.
[84] N. H. Cohrs, K. Schulz-Schönhagen, F. Jenny, D. Mohn, W. J. Stark, *J. Mater. Sci.* **2017**, *52*, 9023.
[85] S. Tansaz, L. Liverani, L. Vester, A. R. Boccaccini, *Mater. Lett.* **2017**, *199*, 143.
[86] J. E. Karbowniczek, D. P. Ura, U. Stachewicz, *Composites, Part B* **2022**, *241*, 110011.
[87] E. Otsuka, A. Yamaguchi, S. Hirose, H. Hagiwara, *Am. J. Physiol. Cell Physiol.* **1999**, *277*, 46.
[88] M. Koike, H. Shimokawa, Z. Kanno, K. Ohya, K. Soma, *J. Bone Miner. Metab.* **2005**, *23*, 219.
[89] J. C. Robins, N. Akeno, A. Mukherjee, R. R. Dalal, B. J. Aronow, Y. H. Koh, P. Koopman, T. L. Clemens et al., *Bone* **2005**, *37*, 313.
[90] J. Ding, K. Nagai, J. T. Woo, *Biosci. Biotechnol. Biochem.* **2003**, *67*, 314.
[91] J. Huang, L. Zhao, L. Xing, D. Chen, *Stem Cells* **2010**, *28*, 357.

 © 2025 The Author(s). Advanced Engineering Materials published by Wiley-VCH GmbH

15272648, 2025, 4, Downloaded from https://advanced.onlinelibrary.wiley.com/doi/10.1002/adem.202500946, By Marta Miola - Politecnico Di Torino Sist. Bibl Del Polit Di Torino, Wiley Online Library on [12/03/2026]. See the Terms and Conditions (https://onlinelibrary.wiley.com/terms-and-conditions) on Wiley Online Library for rules of use; OA articles are governed by the applicable Creative Commons License